

1 **Supplementary data**

2  
3 **Neural stem cells secrete factors facilitating brain regeneration upon constitutive**  
4 **Raf-Erk activation**

5  
6 (Running title: Therapeutic use of Raf-Erk activation in NSCs)

7  
8  
9 Yong-Hee Rhee<sup>1,2,8</sup>, Sang-Hoon Yi<sup>1,2,8</sup>, Joo Yeon Kim<sup>3</sup>, Mi-Yoon Chang<sup>1,2</sup>, A-Young Jo<sup>1,2</sup>, Jinyoung  
10 Kim<sup>1,2</sup>, Chang-Hwan Park<sup>2,5</sup>, Je-Yoel Cho<sup>6</sup>, Young-Jin Choi<sup>7</sup>, Woong Sun<sup>3</sup>, Sang-Hun Lee<sup>1,2,5,8</sup>

11  
12  
13 <sup>1</sup>Department of Biochemistry and Molecular Biology, College of Medicine, Hanyang University,  
14 Seoul, Korea

15 <sup>2</sup>Hanyang Biomedical Research Institute, Hanyang University, Seoul, Korea

16 <sup>3</sup>Department of Anatomy, College of Medicine, Korea University, Seoul, Korea

17 <sup>4</sup>Department of Microbiology, College of Medicine, Hanyang University, Seoul, Korea

18 <sup>5</sup>Graduate School of Biomedical Science and Engineering, Hanyang University, Seoul, Korea

19 <sup>6</sup>Department of Biochemistry, BK21 PLUS Program for Creative Veterinary Science Research and  
20 Research Institute for Veterinary Science, College of Veterinary Medicine, Seoul National  
21 University, Seoul, South Korea

22 <sup>7</sup>ProtAnBio, Co., Seoul, South Korea

23 <sup>8</sup>Co-first author

24  
25  
26 **§Author for correspondence**

27 Department of Biochemistry and Molecular Biology

28 College of Medicine, Hanyang University

29 Seoul, KOREA

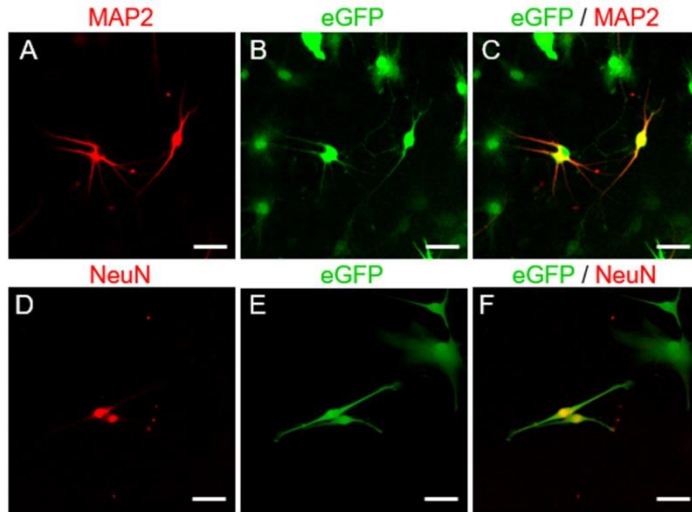
30 Phone: 82-2-2220-0625

31 Email: [leesh@hanyang.ac.kr](mailto:leesh@hanyang.ac.kr)

1 **Supplementary Figures and legends**

2

3 **Figure S1**

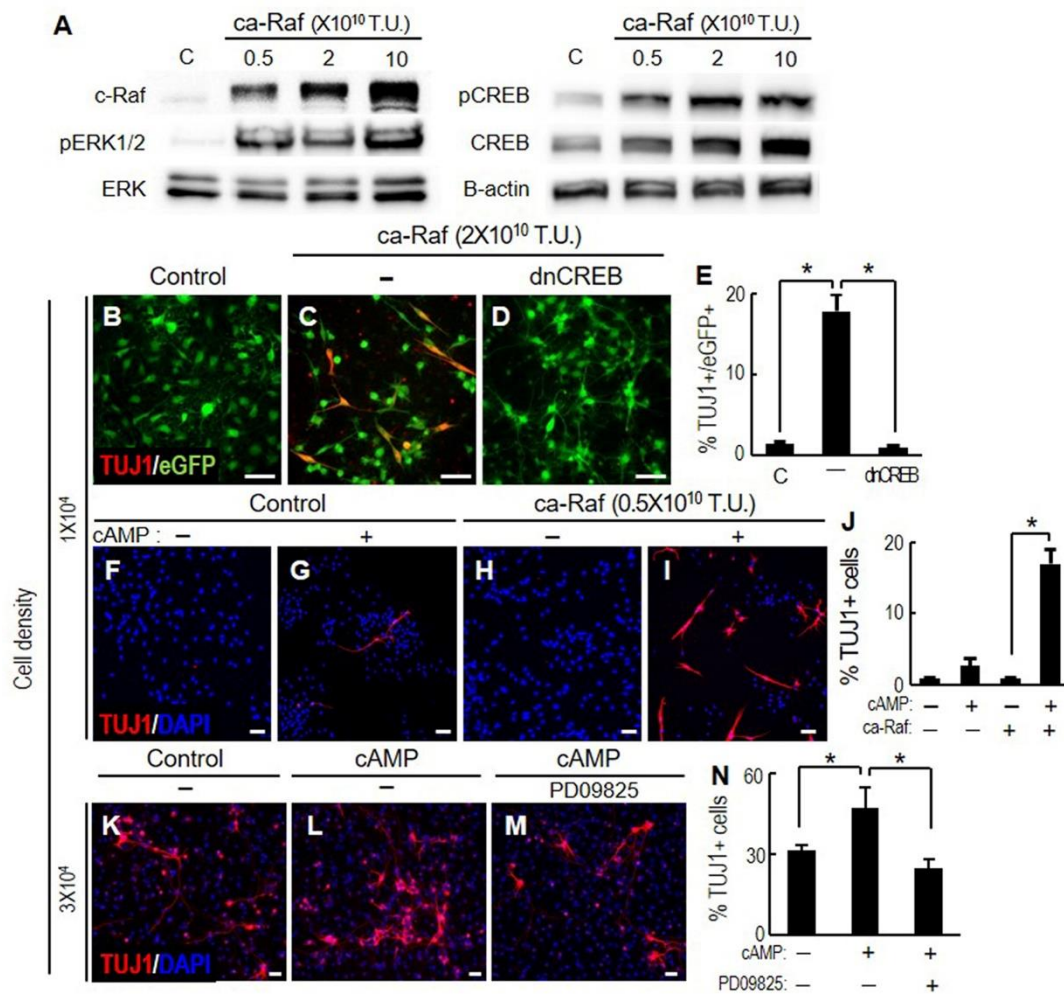


4

5 **Fig. S1.** Expression of the mature neuron-specific markers MAP2 (A-C), NeuN (D-F) in Raf-  
6 transduced eGFP+ cells. NSCs derived from rat embryonic cortices were plated at  $5 \times 10^3$  cells /cm<sup>2</sup>  
7 and transduced with bicistronic *ca-Raf-IRES-eGFP* ( $2 \times 10^{10}$ TU). The low density cultures were  
8 differentiated for 10 days and then immunostained against eGFP/MAP2 and eGFP/NeuN. Scale bar,  
9 30µm.

10

1 **Figure S2**

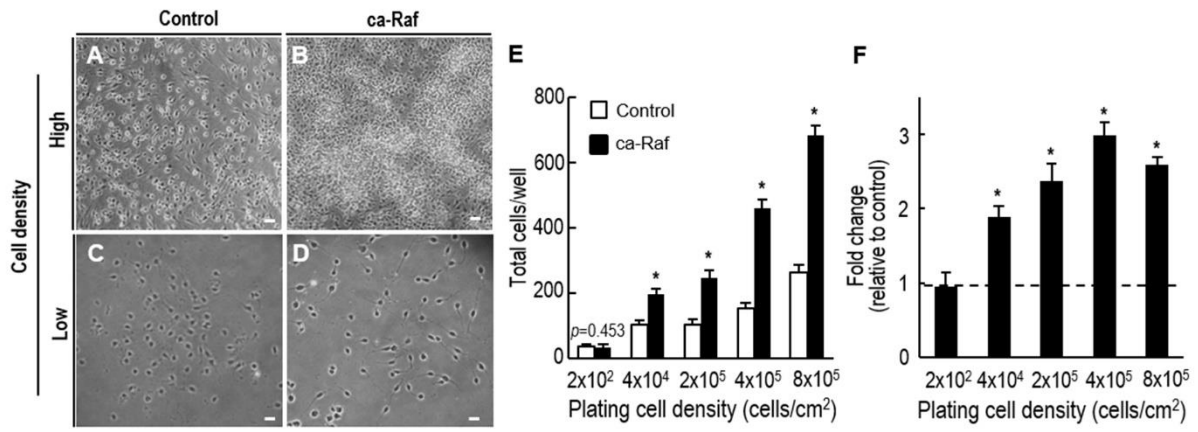


2

3 **Fig. S2.** CREB mediates neuronal differentiation induced by Raf-Erk activation. E14 cortical NSCs  
 4 were plated at 1x (B-J) or 3x10<sup>4</sup>/cm<sup>2</sup> (A and K-N), and transduced (or not) the following day.  
 5 Analyses were carried out 4-6 days after transduction. A, CREB activation estimated from  
 6 phosphorylated CREB (pCREB) protein levels obtained by WB analysis. B-E, CREB inhibition  
 7 abolishes neuronal differentiation induced by ca-Raf expression. TUJ1<sup>+</sup> neuronal yields were  
 8 estimated in cultures transduced with empty control (B), ca-Raf (C), and ca-Raf+ dominant negative  
 9 CREB (dn-CREB) (D). The transduced cells were labeled with *eGFP* using the bicistronic *-IRES-*  
 10 *eGFP* construct. F-J, cAMP treatment enhances ca-Raf-induced neuronal yields. K-N, cAMP-induced  
 11 neuron formation is abolished by the Erk inhibitor PD98059 (10μM). \**p*<0.005, n=3-5 cultures for  
 12 each group, one-way ANOVA. Scale bars, 50μm.

13

1 **Figure S3**



2

3 **Fig. S3.** Cell density-dependent effect of Raf-Erk activation on cell proliferation. Cortical NSCs were  
 4 plated at the cell densities indicated, and transduced with ca-Raf or mock control the following day.

5 The cultures were fixed and total viable cells were counted 4 days after transduction. A-D,

6 Representative phase contrast images 4 days after cell plating at 4x10<sup>5</sup> cells/cm<sup>2</sup> (high) and 2x10<sup>2</sup>

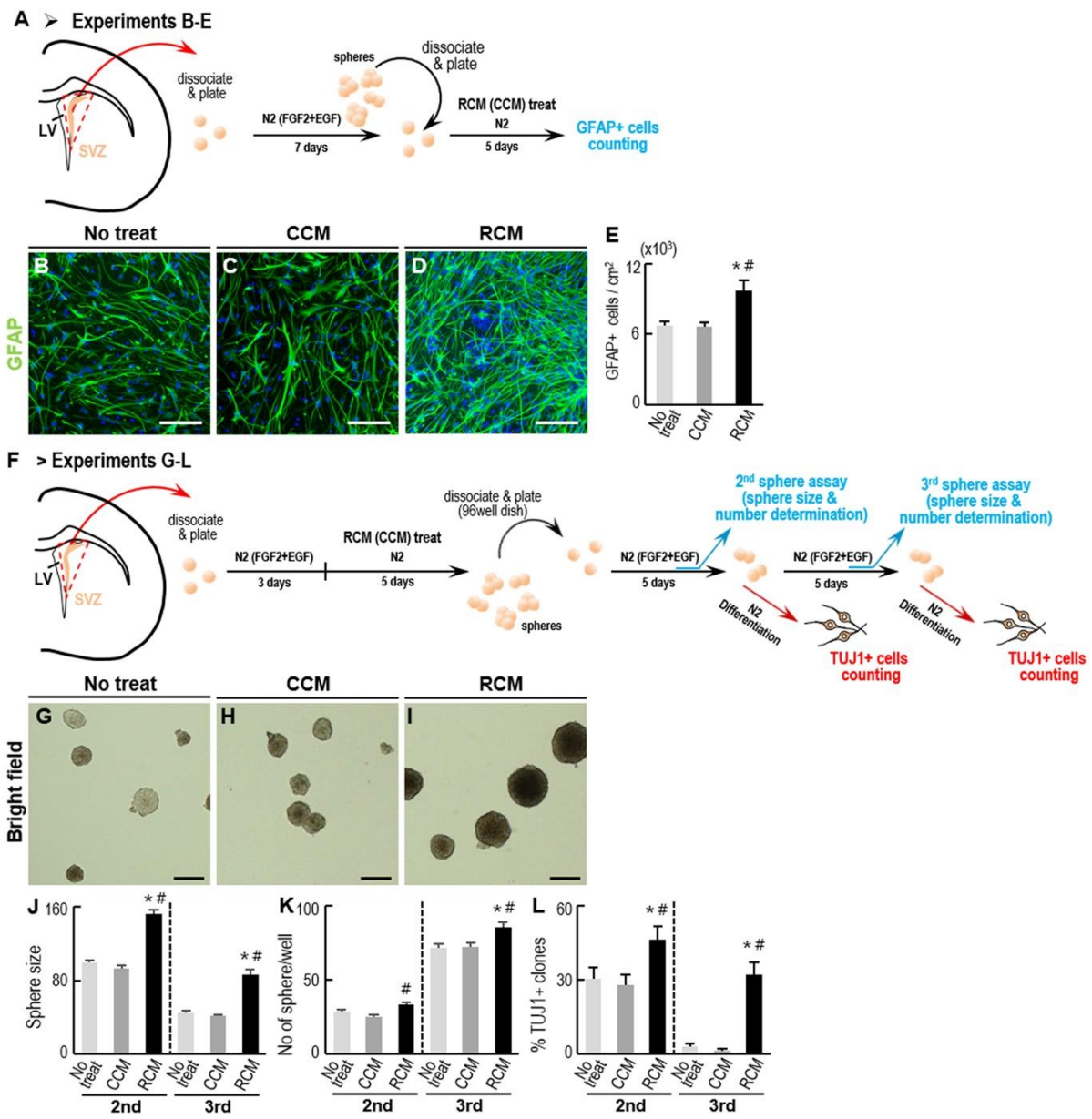
7 cells/cm<sup>2</sup> (low). E and F, The data are total cells/well (E) and % cell numbers relative to the respective

8 controls (F) at each cell density. \**p*<0.01, n=3 culture wells for each datum, one-way ANOVA. Scale

9 bars, 50μm.

10

1 **Figure S4**



2

3 **Fig. S4.** The effect of RCM on adult brain-derived NSCs. A-E, RCM effect on GFAP+ adult NSC

4 number. A, schematic of the experimental procedure in B-E. Cells dissociated from the SVZs were

5 cultured in N2 supplemented with FGF2+EGF (20 ng/ml each) for 7 days. The spheres formed were

6 dissociated, plated on PLO/FN-coated dishes, and cultured in N2 medium in the presence of CM or

7 not. Five days later, GFAP+ cells were estimated (B-E). Significantly different from the untreated\*

8 and from the CCM-treated# at  $p < 0.001$ ,  $n = 3$  culture wells. F-L, Neurosphere-forming assays.

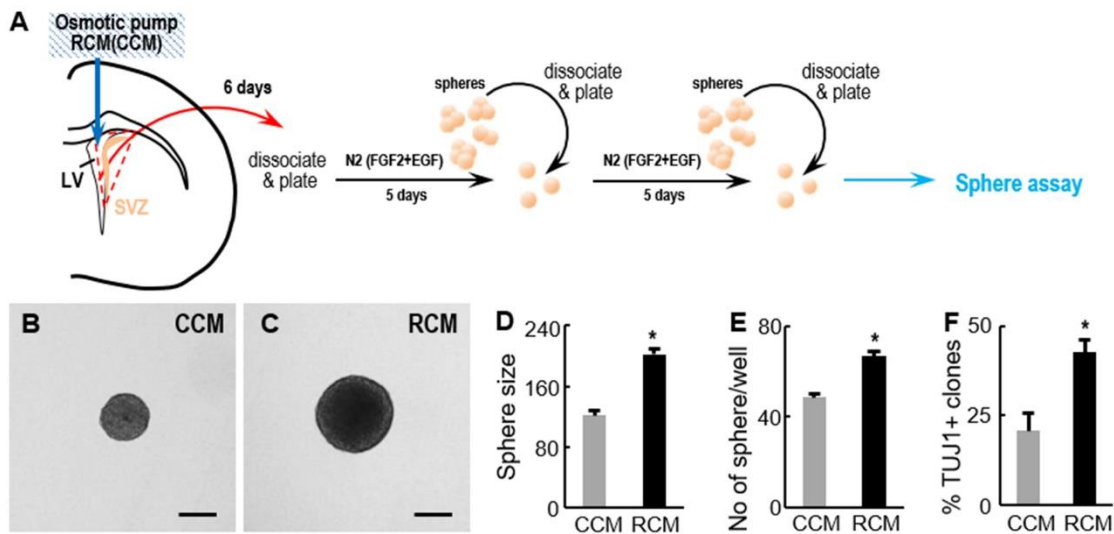
9 Schematic of the experimental procedure is shown in F. SVZ-derived neurospheres were treated with

10 CM for 5 days, then dissociated into single cells, and plated at 150 cells/well in 96-well plates. The

1 sizes and numbers of spheres (secondary) formed after 5 days were assessed (G-J). The secondary  
2 spheres were collected and subjected to tertiary sphere forming assays in the same way. The  
3 secondary and tertiary spheres were attached to PLO/FN-coated dishes and induced to differentiate in  
4 N2 medium. % TUJ1+ colonies were counted after 7 days (L). 120 spheres (J), 40 wells (K), 6 dishes  
5 (L) were analyzed. Significantly different from the untreated\* and from the CCM-treated# at  $p < 0.001$ ,  
6 one-way ANOVA. Scale bar, 100 $\mu$ m.

7

1 **Figure S5**



2

3 **Fig. S5.** Sphere forming assays using RCM (or CCM)-infused SVZs. A, RCM (or CCM) were infused

4 into the right LV of adult mice (without TBI) as described in Fig. 5A. Six days after infusion, the

5 ipsilateral SVZs were dissociated and cultured in FGF2 + EGF-supplemented N2 for 5 days. Spheres

6 formed were dissociated into single cells and neurosphere-forming assays were carried out as

7 described in Supplementary Fig. S4. B-F, Sizes (D) and numbers (E) of the spheres were assessed 5

8 days after plating on 96-well plates. Shown in B and C are representative spheres derived from CCM-

9 and RCM-infused SVZ tissues, respectively. The spheres were plated on PLO/FN-coated dishes and

10 induced to differentiate in N2 medium. TUJ1+ neuron-containing clones were counted 7 days after

11 differentiation (F). 40 spheres (D), 30-40 wells (E), and 200-300 clones (F) were analyzed per animal,

12 and the data are expressed as mean  $\pm$  SEM of 3 mice. \*Significantly different from CCM-infused

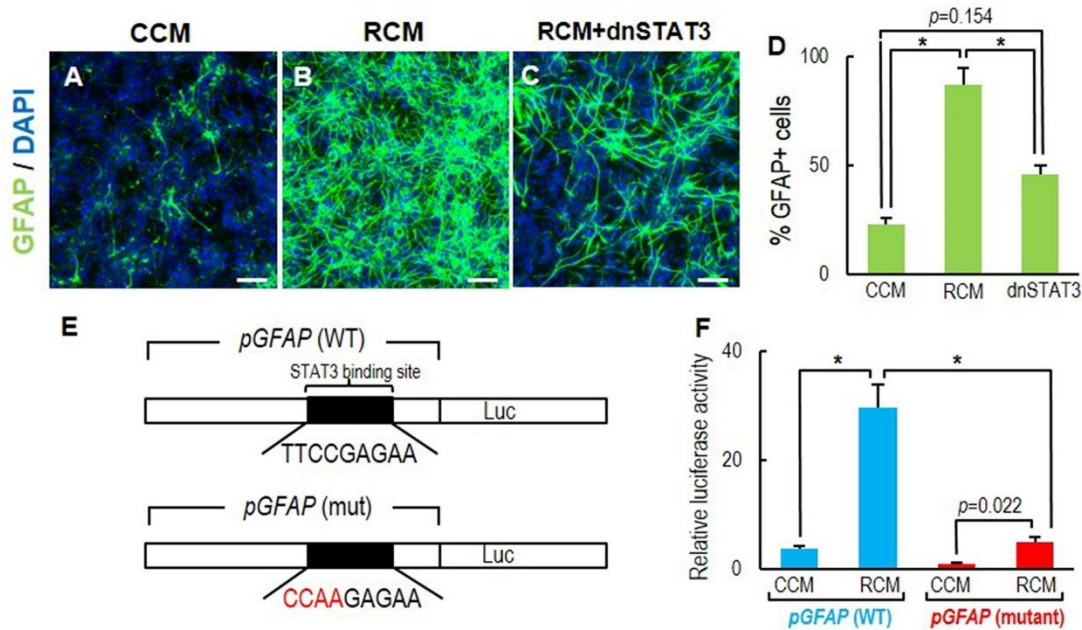
13 mice at  $p < 0.001$ , Student's t-test,  $n = 3$  mice for each RCM- and CCM-infused group. Scale bar,

14 200 $\mu$ m.

15



1 **Figure S6**

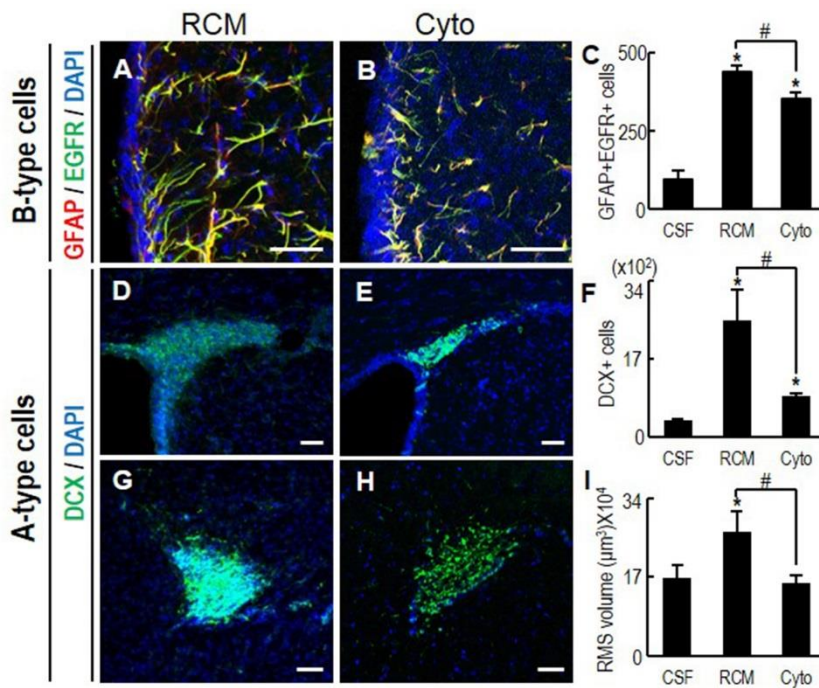


2  
3 **Fig. S6.** Jak-STAT signal activation is responsible for astrocytic differentiation induced by RCM  
4 treatment. A-D, Enhanced astrocyte yields in RCM-treated cultures are abolished by STAT signal  
5 inhibition using a dominant negative STAT3 (dn-STAT3). NSCs cultured from cortices of rat embryos  
6 (at E14) were transduced with retroviruses expressing dn-STAT3 (C) or mock vector (A, B). Two days  
7 after transduction, the NSCs were treated with CCM or RCM for 4 days. GFAP+ cells were counted 4  
8 days after CM treatment (D). \* $p < 0.001$ ,  $n = 3$  cultures, one way-ANOVA. scale bar, 50 $\mu$ m. E and F,  
9 *GFAP* promoter assay. Schematic drawing of the STAT binding sequences in the luciferase reporters  
10 driven by the wild-type (WT) and mutant (mut) *GFAP* promoters (*pGFAP*) (E). The cortical NSCs  
11 were transfected with the reporter vectors and luciferase activities were determined in (F). \* $p < 0.001$ ,  
12  $n = 4$  replicates, one way-ANOVA.

13



1 **Figure S7**



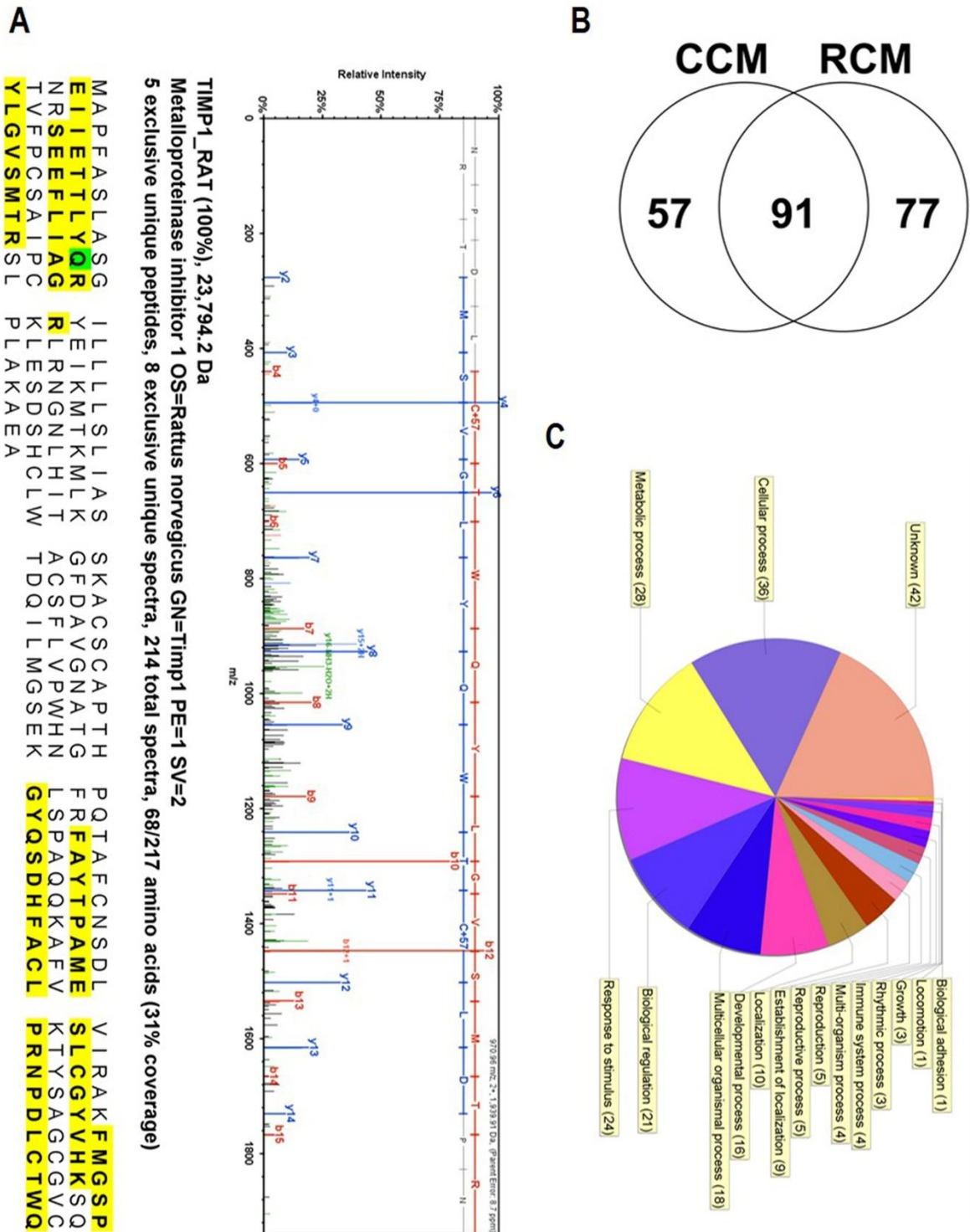
2

3 **Fig. S7.** Effect of the combined cytokines LIF+FGF2+VEGF on in vivo neurogenesis by SVZ-NSCs.

4 The levels of the cytokines LIF, FGF2, and VEGF were determined as described in Fig.7P and they  
 5 were infused as described in Fig.5A. Cell populations of activated B-type cells (GFAP/EGFR- double  
 6 positive, A-C) in the SVZ and A cells (DCX+) in the SVZ (D-F) and RMS (G-I) of the cytokine-  
 7 infused (Cyto) brains were compared with those of the mice infused with CSF (control) and RCM.  
 8 Significantly different from the CSF-infused control\* and from the RCM-infused# at  $p < 0.005$ , one-  
 9 way ANOVA,  $n = 4$  (CSF), 7 (RCM), and 4 (Cyto). Scale bar, 50µm.

10

1 **Figure S8**

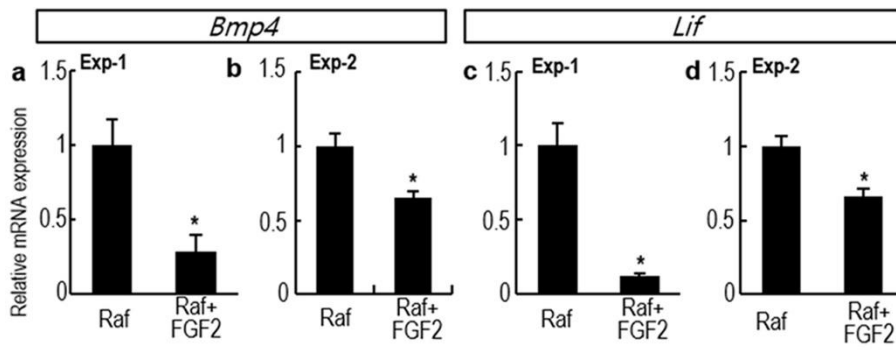


2  
 3 **Fig. S8.** Identification of proteins in CM by LC-MS/MS. Proteins (100µg) in RCM and CCM were  
 4 separated by 12% SDS-PAGE and stained with Coomassie Brilliant Blue. The stained proteins were  
 5 cut into 20 pieces for in-gel trypsin digestion and analyzed. A, Representative LC/MS spectrum of the  
 6 metalloproteinase inhibitor 1 (TIMP1) identified in RCM. B, Band-diagram exhibiting numbers of the

1 proteins detected in RCM and CCM. A total 225 proteins were identified, of which 57 and 77 proteins  
2 were detected only in the CCM and RCM, respectively, and 91 proteins were detected in both the  
3 CCM and RCM. C, Ontologic analysis of the 77 proteins present only in RCM and 6 proteins that  
4 were >5 fold higher in RCM than CCM (listed in Table S2). The proteins are classified according to  
5 the gene ontology term: "Biological process".

6

1 **Figure S9**



2

3 **Fig. S9.** Real-time PCR analysis of *Bmp4* and *Lif* mRNA expression in ca-Raf-transduced NSC

4 cultures in the presence or absence of FGF2 (10 ng/ml). \*Significant at  $p < 0.01$ ,  $n = 3$  PCR reactions for

5 each datum, Student's t-test.

6

1 Table. S1. Primers for PCR analyses, Related to Figure 4.

2

<b>Gene symbol</b>	<b>Sequence</b>
<i>Aqp4</i>	F: TTG CTT TGG ACT CAG CAT TG
	R: GGG AGG TGT GAC CAG GTA GA
<i>Bmp2</i>	F: TGA GGC TGC TCA CCA TGT TTG
	R: GTG ACA TCA AAG CTC TCC CAC T
<i>Bmp4</i>	F: ATT GGC TCC CAA CTT CTT CCT TT
	R: CGT GAT GGA AAC TCC TCA CAG T
<i>Bmp7</i>	F: CGC TCC AAG ACT CCA AAG AAC C
	R: CGG TGT CTG GGT TGATGA AGT G
<i>Egfr</i>	F: ACC GTG GAG AGA ATC CCT TT
	R: TTG TTG CTA AAT CGC ACA GC
<i>Fabp7</i>	F: CCA GCT GGG AGA AGA GTT TG
	R: TAA CAG CGA ACA GCA ACG AC
<i>Fgf1</i>	F: CGC AGA CAC CAA ATG AAG AA
	R: TTT CTG GCC GTA GTG AGT CC
<i>Fgf2</i>	F: GAA CCG GTA CCT GGC TAT GA
	R: CCG TTT TGG ATC CGA GTT TA
<i>Gapdh</i>	F: GGC ATT GCT CTC ATT GAC AA
	R: AGG GCC TCT CTC TTG CTC TC
<i>Gfap</i>	F: GCA GAC CTC ACA GAC GTT GCT
	R: AGG CTG GTT TCT CGG ATC TGG
<i>Slc1a3</i>	F: GGA TGG AAA GA TTC CAG CAA
	R: ACC TCC CGG TAG CTC ATT TT
<i>Glt1</i>	F: CCA AAA GCA ACG GAG AAG AG
	R: ACC TCC CGG TAG CTC ATT TT
<i>Lif</i>	F: GGC AAC CTC ATG AAC CAG AT
	R: ACC ATC CGA TAC AGC TCG AC
<i>Nestin</i>	F: GGA GTG TCG CTT AGA GGT
	R: TCC AGA AAG CCA AGA GAA
<i>Notch</i>	F: GGT GCG AGC GCA GTG AAG GA
	R: CCC GCT GCT GCC CTC TTT CC
<i>Sox2</i>	F: TCA CAA CAA TCG CGG CGG CCC
	R: GCG CGG AGA TCT GGC GGA GAA T
<i>Pax6</i>	F: TGT CCA ACG GAT GTG TGA GT
	R: TTT CCC AAG CAA AGA TGG AC
<i>Vegf</i>	F: GTG CAC TGG ACC CTG GCT TTA CT
	R: CGC CTT GCA ACG CGA A
<i>Vimentin</i>	F: AGA TCG ATG TGG ACG TTT CC
	R: CAC ACT GTC TCC GGT ATT CGT

3

4

1 Table. S2. Proteins abundantly detected in the RCM, Related to Figure S8.

2

#	Identified Proteins	Accession Number	Fold change by sample	Normalized Spectral counts	
				CCM	RCM
1	Vimentin OS	G3V8C3_RAT (+1)	RCM only		125
2	Metalloproteinase inhibitor 1	TIMP1_RAT	RCM only		160
3	Alpha-2-macroglobulin	A2MG_RAT	RCM only		114
4	Moesin	A0A096MK30_RAT(+1)	RCM only		51
5	Peptidyl-prolyl cis-trans isomerase	Q6AYQ9_RAT	RCM only		93
6	Sulfated glycoprotein 1	F7EPE0_RAT (+1)	RCM only		49
7	Mannan-binding lectin serine protease 1	MASP1_RAT	RCM only		56
8	Carbonic anhydrase 2	CAH2_RAT	RCM only		65
9	Uncharacterized protein	D3ZJE2_RAT (+1)	RCM only		57
10	Gelsolin	GELS_RAT	RCM only		37
11	Myosin-6	MYH6_RAT	RCM only		1
12	Histone H3	D3ZJ08_RAT (+6)	RCM only		13
13	Uncharacterized protein (Fragment)	F1M9P7_RAT (+1)	RCM only		43
14	Chloride intracellular channel protein 1	CLIC1_RAT	RCM only		47
15	Heat shock protein HSP 90-alpha	HS90A_RAT	RCM only		43
16	Nucleolin	NUCL_RAT (+1)	RCM only		19
17	Latexin	LXN_RAT	RCM only		16
18	Elongation factor 1-gamma	EF1G_RAT	RCM only		13
19	Heterogeneous nuclear ribonucleoprotein K	HNRPK_RAT (+2)	RCM only		14
20	Coactosin-like protein	COTL1_RAT	RCM only		6
21	Insulin-like growth factor-binding protein 3	IBP3_RAT	RCM only		21
22	Dextrin	DEST_RAT	RCM only		78
23	Amyloid beta A4 protein	A4_RAT	RCM only		6
24	Eukaryotic translation initiation factor 5A2 (Predicted)	G3V7J7_RAT (+1)	RCM only		4
25	Elongation factor 1-alpha 1	EF1A1_RAT	RCM only		17
26	Glutathione S-transferase alpha-4	GSTA4_RAT	RCM only		5
27	Proteasome subunit beta type	G3V8U9_RAT (+1)	RCM only		10
28	Proteasome subunit beta type-2	PSB2_RAT	RCM only		2
29	60S acidic ribosomal protein P0	RLA0_RAT	RCM only		25
30	Ubiquitin-conjugating enzyme E2 N	UBE2N_RAT	RCM only		12
31	Poly(RC) binding protein 2	Q6AYU5_RAT	RCM only		25
32	Pyruvate kinase PKM	KPYM_RAT	RCM only		18
33	Protein LOC100362142	D3ZFY8_RAT	RCM only		25
34	Protein Snrpd3	M0R907_RAT	RCM only		4
35	Prothymosin alpha	PTMA_RAT	RCM only		19
36	Actin related protein 2/3 complex, subunit 4 (Predicted), isoform CRA_a	B2RZ72_RAT	RCM only		13
37	Carbonyl reductase [NADPH] 1	CBR1_RAT (+1)	RCM only		7
38	Thioredoxin (Fragment)	R4GNK3_RAT (+1)	RCM only		9

39	14-3-3 protein eta	I433F_RAT	RCM only	90
40	Adenylate kinase 2	KAD2_RAT	RCM only	13
41	Heterogeneous nuclear ribonucleoprotein F	HNRPF_RAT	RCM only	16
42	Prostaglandin E synthase 3 (Fragment)	R9PXR7_RAT (+1)	RCM only	5
43	Protein Eea1 (Fragment)	F1LUA1_RAT	RCM only	1
44	Protein LOC100910754	D4A0F5_RAT (+2)	RCM only	2
45	Plastin 3 (T-isoform), isoform CRA_a	F1LPK7_RAT (+1)	RCM only	12
46	Protein Hectd4 (Fragment)	F1LZX5_RAT	RCM only	4
47	NudC domain-containing protein 2	NUDC2_RAT (+1)	RCM only	7
48	Protein Dag1	F1M8K0_RAT	RCM only	4
49	Protein Tln1	G3V852_RAT	RCM only	1
50	RCG50226, isoform CRA_a	G3V8P4_RAT	RCM only	4
51	Actin-related protein 2/3 complex subunit 3	B2GV73_RAT	RCM only	7
52	6-phosphogluconolactonase	6PGL_RAT (+1)	RCM only	8
53	Proteasome subunit beta type	F1LNN1_RAT (+1)	RCM only	2
54	Clathrin heavy chain 1	CLH1_RAT (+1)	RCM only	1
55	Cullin-associated NEDD8-dissociated protein 1	CAND1_RAT	RCM only	4
56	Keratin, type II cytoskeletal 1	K2C1_RAT	RCM only	7
57	Protein Sh3bgrl3	B2RZ27_RAT	RCM only	2
58	Protein Ppp2r1a	Q5XI34_RAT	RCM only	1
59	Heterogeneous nuclear ribonucleoprotein C	G3V9R8_RAT	RCM only	10
60	Alpha-actinin-4	ACTN4_RAT	RCM only	2
61	Peptidyl-prolyl cis-trans isomerase D	PPID_RAT	RCM only	8
62	UMP-CMP kinase	KCY_RAT	RCM only	1
63	Uncharacterized protein (Fragment)	F1LYE1_RAT	RCM only	1
64	72 kDa type IV collagenase	E9PSM5_RAT (+1)	RCM only	7
65	Protein LOC102547754	D4ADL2_RAT	RCM only	2
66	Thimet oligopeptidase	THOP1_RAT	RCM only	2
67	Protein LOC100360057 (Fragment)	F7FLF2_RAT (+1)	RCM only	4
68	Importin subunit beta-1	F2Z3Q8_RAT (+1)	RCM only	4
69	Nidogen-1	F1LM84_RAT	RCM only	2
70	Clusterin	CLUS_RAT (+1)	RCM only	4
71	Serine/threonine-protein phosphatase PP1-alpha catalytic subunit	PP1A_RAT	RCM only	2
72	Protein Chd4	E9PU01_RAT	RCM only	1
73	Heterogeneous nuclear ribonucleoprotein D, isoform CRA_b	G3V6A4_RAT (+3)	RCM only	2
74	Glutathione S-transferase omega-1	GSTO1_RAT (+1)	RCM only	2
75	Ubiquitin-conjugating enzyme E2 variant 2	UB2V2_RAT	RCM only	3
76	Protein Sorcs1	F1LUZ4_RAT	RCM only	1



<b>77</b>	Protein LOC100362339	D4A6G6_RAT (+1)	RCM only		1
<b>78</b>	Carboxypeptidase E	CBPE_RAT	9.1	20	179
<b>79</b>	Glia-derived nexin	G3V7Z4_RAT	8.6	55	469
<b>80</b>	SPARC-like 1 (Mast9, hevin), isoform CRA_a	G3V7X5_RAT (+1)	7.2	64	457
<b>81</b>	Transketolase	G3V826_RAT (+1)	6.9	9	63
<b>82</b>	Insulin-like growth factor-binding protein 2	IBP2_RAT	6.5	41	264
<b>83</b>	Heat shock cognate 71 kDa protein	HSP7C_RAT	6.4	21	136

1

2